

# ADAPTIVE FILTERING OF FMRI DATA BASED ON CORRELATION AND BOLD RESPONSE SIMILARITY

J. Rydell, H. Knutsson, M. Borga

Department of Biomedical Engineering, Linköping university, Sweden

Center for Medical Image Science and Visualization (CMIV), Linköping university, Sweden

## ABSTRACT

In analysis of fMRI data, it is common to average neighboring voxels in order to obtain robust estimates of the correlations between voxel time-series and the model of the signal expected to be present in activated regions. We have previously proposed a method where only voxels with similar correlation coefficients are averaged. In this paper we extend this idea, and present a novel method for analysis of fMRI data. In the proposed method, only voxels with similar correlation coefficients and similar time-series are averaged. The proposed method is compared to our previous method and to two well-known filtering strategies, and is shown to have superior ability to discriminate between active and inactive voxels.

## 1. INTRODUCTION

Analysis of functional MRI data deals with the problem of detecting very weak signals in very noisy data. The common solution to this problem is to average the time series from neighboring pixels or voxels, and thereby enhance the signal to noise ratio [1]. In practice, this is done by convolving the slices (or volumes) with a fixed low-pass filter kernel, e.g. a gaussian. The price to pay for this kind of noise reduction is loss of spatial resolution. Loss of spatial resolution means that the shape of activated regions cannot be accurately determined and, perhaps worse, that small activated regions may remain undetected.

In order to maintain high spatial resolution, the spatial low-pass filtering can be made *adaptive* and *non-isotropic*. This means that for each voxel, the size and shape of the local region, in which the averaging is performed, is data dependent. A method for adaptive spatial filtering based on canonical correlation analysis (CCA) has previously been suggested [2]. That method chooses the size and shape of the local averaging region, i.e. the resulting adaptive filter, such that the *correlation* between the averaged time series and the model of the blood oxygen level dependent (BOLD) response model is maximized. This makes the method very sensitive. Indeed, the method is so sensitive that restrictions have to be imposed on the number of parameters in the adaptive filter and their

ranges in order to maintain a reasonable selectivity. If given too much freedom, the method may find false signals in the noise since the filter is optimized for making the filter output as similar to the BOLD response model as possible. Another problem with this method is that when the filter is centered in a non-activated voxel but close to an activated region, the filter will try to "reach in" to the activated region in order to pick up as much activation as possible. This will make the resulting regions labeled as active become larger than they should be, i.e. a growing of activated regions will occur.

We have previously proposed an alternative method for adaptive filtering [3]. That method is based on averaging of voxels which have similar correlation with the BOLD model, and has the advantage that edges between active and inactive regions are preserved. We here present an extension of this filtering scheme, where voxels to be averaged are not only required to have similar correlation with the BOLD model, but should also have similar time-series. We also show that this modification provides a significant improvement of the detection performance.

## 2. THEORY

When ordinary low-pass filtering is used for noise reduction, voxels that are spatially close to each other are treated as samples from one distribution, and a weighted average of the voxels in a neighborhood is used as an estimate of the true signal value in the center of that region. The weights are predetermined and based on the distance from the center of the neighborhood. Close to edges in an image, the voxel values are actually samples from two or more distributions, and using predetermined weights for averaging causes blurring of the edges. Bilateral filtering [4, 5] extends low-pass filtering by also considering the distance between the value of a certain voxel and that of the center voxel, thereby creating a different filter kernel in each neighborhood. This approach causes voxels from the other side of an edge to be treated as outliers, and thus their effect on the estimate of the true signal value is reduced or eliminated. An example of using low-pass filtering and bilateral filtering, respectively, of a noisy one-dimensional signal is shown in figure 1. The signal is a step function with additive gaussian noise, and it is obvious

---

Thanks to the Swedish Research Council for funding.

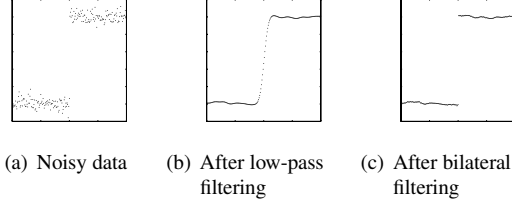


**Fig. 1.** Noisy data before and after low-pass and bilateral filtering.

that low-pass filtering causes blurring of the edge while it is preserved by bilateral filtering.

The bilateral filter kernel in each neighborhood can be expressed as a product of two filter kernels: the spatial filter  $F_s$  and the range filter  $F_r$ . The spatial filter is based on spatial distance, and corresponds to the filter kernel used in low-pass filtering, while the range filter is based on the difference in image intensity. That is, given an image  $I(x, y)$ , the bilateral filter kernel  $F(\Delta x, \Delta y)$  at image coordinates  $(x, y)$  can be written

$$F(\Delta x, \Delta y) = F_s(\Delta x, \Delta y) \cdot F_r(\Delta x, \Delta y) \quad (1)$$

where  $F_s(\Delta x, \Delta y)$  is an ordinary spatial filter kernel  $g(\Delta x, \Delta y)$  and the range filter is defined as

$$F_r(\Delta x, \Delta y) = h(I(x + \Delta x, y + \Delta y) - I(x, y)) \quad (2)$$

A common choice of the filter kernels  $g$  and  $h$  is gaussian functions.

### 3. METHOD

Godtliebsen et al [6] have proposed using bilateral filtering of the raw fMRI data, with a time dimension in addition to the spatial and range dimensions described above. Our previous method is similar to bilateral filtering, but instead of basing the range filter on differences in image intensity, we base it on the difference in correlation between individual voxel time-series and the BOLD model. Furthermore, instead of using the correlation coefficients directly, we use a mapping of the correlation. The reason for using this mapping is that the correlation coefficients are not readily comparable on a linear scale. The mapping is defined as

$$\Lambda(x, y) = \log\left(\frac{1}{1 - \rho(x, y)^2}\right) \quad (3)$$

where  $\rho(x, y)$  is the correlation between the time-series at coordinates  $(x, y)$  and the BOLD model. Under certain conditions this measure, which is the logarithm of Wilks' lambda, is equivalent to mutual information.

Here we propose an extension of the previous method, where we use *two* range filters. One of these ( $F_{r_1}$ ) is identical to the range filter described above, while the other ( $F_{r_2}$ )

is based on the similarity between the intensity time-series themselves. That is, two spatially close voxels are averaged if their individual correlations with the BOLD model are similar *and* their time-series resemble each other.

Often, the BOLD model used in fMRI data analysis is a linear subspace model, i.e. a model with two or more temporal basis signals. The correlation between a time-series and the model is then defined as the highest correlation between the signal and any linear combination of the model basis signals. The model basis can, for example, be generated by performing principal component analysis of a large number of simulated BOLD responses, generated by Buxton's balloon model [7]. We propose that such a subspace model is used, and use the angle between the projections of two time-series onto the model subspace as a measure of similarity between the two time-series. (In experiments with more than one stimuli, a linear subspace model can instead be based on the expected responses from each of the stimuli.) By measuring the angle in the signal subspace, large random variations that are due to the high noise levels in the data are disregarded. If the time-series were directly compared to each other, any similarity would remain undetected because of the noise.

Simply combining the spatial and range filters would, at each coordinate  $(x, y)$ , yield a filter

$$F(\Delta x, \Delta y) = F_s(\Delta x, \Delta y) \cdot F_{r_1}(\Delta x, \Delta y) \cdot F_{r_2}(\Delta x, \Delta y) \quad (4)$$

which averages over voxels that are close to each other, where the correlation with the BOLD model is similar, and where the projection of the signal onto the BOLD model basis functions is similar. However, this is generalized slightly by introducing the parameters  $\alpha$ ,  $\beta$  and  $\gamma$  as follows:

$$F(\Delta x, \Delta y) = F_s(\Delta x, \Delta y)^\alpha \cdot F_{r_1}(\Delta x, \Delta y)^\beta \cdot F_{r_2}(\Delta x, \Delta y)^\gamma \quad (5)$$

These parameters can be used to tune the relative importance of the different filters. The parameters can even be variable, to accommodate different weightings of the filter kernels in different neighborhoods. This makes the proposed method very general. We do, however, here propose specific choices of the parameters.

As was mentioned in the last section, it is common to choose  $F_s$  and  $F_r$  to be gaussian functions. Accordingly, we suggest that all of  $F_s$ ,  $F_{r_1}$  and  $F_{r_2}$  are selected as such. Thus,

$$F_s(\Delta x, \Delta y) = \exp\left(-\frac{d_s(\Delta x, \Delta y)^2}{2\sigma_s^2}\right) \quad (6)$$

$$F_{r_1}(\Delta x, \Delta y) = \exp\left(-\frac{d_{r_1}(\Delta x, \Delta y)^2}{2\sigma_{r_1}^2}\right) \quad (7)$$

$$F_{r_2}(\Delta x, \Delta y) = \exp\left(-\frac{d_{r_2}(\Delta x, \Delta y)^2}{2\sigma_{r_2}^2}\right) \quad (8)$$

where the distance measures are defined as

$$d_s(\Delta x, \Delta y) = \sqrt{\Delta x^2 + \Delta y^2} \quad (9)$$

$$d_{r_1}(\Delta x, \Delta y) = \Lambda(x, y) - \Lambda(x + \Delta x, y + \Delta y) \quad (10)$$

$$d_{r_2}(\Delta x, \Delta y) = \arccos(\hat{\mathbf{w}}(x, y) \cdot \hat{\mathbf{w}}(x + \Delta x, y + \Delta y)) \quad (11)$$

The different  $\sigma$ :s are the standard deviations of the respective gaussian functions and  $\hat{\mathbf{w}}(x, y)$  is the projection direction in the subspace model for the time-series at coordinates  $(x, y)$ .

The values of the exponents  $\alpha$ ,  $\beta$  and  $\gamma$  should be in the range from 0 to 1, where 0 means that the filter has no effect and 1 means that the filter has full effect. This implies that setting  $\alpha = \beta = 1$  and  $\gamma = 0$  yields our previous method as a special case. We propose that these parameters are used as weights for the different filters according to the certainties of their respective distance measures. The exact spatial distance is always known, and thus its certainty  $\alpha = 1$ . There is no good certainty estimate for the correlation, and thus we also propose that  $\beta$  is constant, for example  $\beta = 1$ . However, the certainty of the projection onto the subspace model is related to our estimate of the correlation. The higher the correlation estimate, the more certain the projection direction is. Thus we select

$$\gamma(\Delta x, \Delta y) = \sqrt[4]{|\rho(x, y)\rho(x + \Delta x, y + \Delta y)|} \quad (12)$$

i.e. the square root of the geometric mean of the correlations in the two pixels under consideration. The choice of the square root is not of crucial importance, but it appears to provide a better weighting than using the geometric mean directly. Then, in regions where the correlation is high, the filter based on time-series similarity will be important, while in other regions it will have little or no effect. This is an advantage in both active and inactive regions. In inactive regions, the correlation is low and the similarity between the time-series is random. By ignoring the second range filter ( $F_{r_2}$ ) in these regions, the final filter will average over larger areas, thus reducing the probability of finding spurious correlations in the noise. In these regions,  $F_{r_1}$  precludes filters that would pick up signal from activated voxels. In active regions, on the other hand, the correlations are higher and thus  $F_{r_2}$  has effect. This decreases the risk of extending the effective filter beyond the active region.

An example of the different filter kernels is shown in figure 2. Figure 2a shows where activity has been embedded in the noise in an artificial data set. In figure 2b, the spatial filter  $F_s$  is shown. Figures 2c and d show the range filters  $F_{r_1}$  and  $F_{r_2}$  when they are located in the dashed square in figure 2a. In this case, the center pixel is located in an activated region. It is clear that the two range filters complement each other, excluding pixels outside of the activated region from the averaging. In figure 2e the resulting filter obtained by combining  $F_s$ ,  $F_{r_1}$  and  $F_{r_2}$  according to equation 5 is shown. The coefficients in this filter are used as weights for averaging the

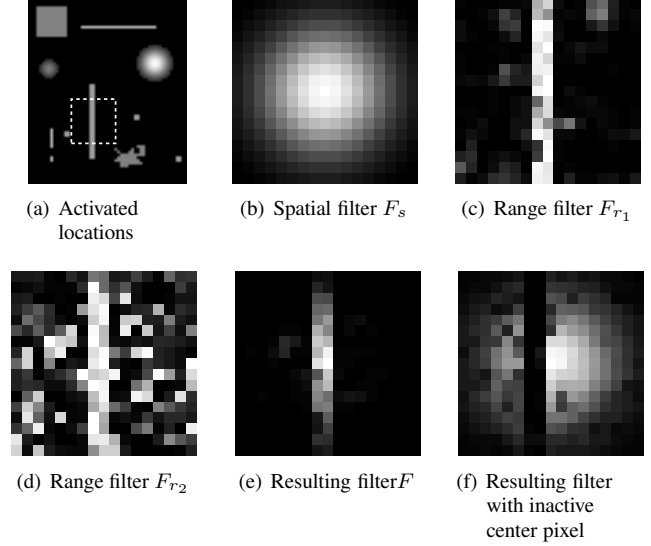


**Fig. 2.** Example of filter kernels based on the different distance measures, and final filter combined using equation 5. The resulting filter in figure e is used for weighting the time-series in the region surrounded by the dashed line in figure a.

time-series in the marked region. As can be seen in the figure, the filter has almost zero weight for inactive pixels but large weights for spatially close pixels with activation similar to that of the center pixel. If the center pixel had been located beside the active region, a filter with large weights for inactive pixels and small weights for active pixels would instead have been obtained. Such a resulting filter, where the center pixel is just outside of the active part of the marked region in figure 2a, is shown in figure 2f.

When the filters  $F(\Delta x, \Delta y)$  have been created at each coordinate  $(x, y)$ , they are used to filter the raw data in each timepoint. After this, each time-series in the resulting data is analyzed separately to detect activation.

It is important to notice that this is different from calculating the correlation in each pixel and then performing bilateral filtering of the correlation map.

## 4. RESULTS AND DISCUSSION

The proposed method has been evaluated on both real and synthetic data. Figures 3b-e show correlation maps generated by analyzing simulated data using fixed low-pass filtering, adaptive filtering using CCA, adaptive filtering using our previous method and adaptive filtering using the proposed method, respectively. The areas where BOLD-like signals were embedded in the noise are shown in figure 3a. The signal to noise ratio of the simulated data is approximately 5 – 10 %. Brighter regions in figure 3a have higher SNR. The noise is gaussian, with spatial autocorrelation similar to that found in real fMRI data.

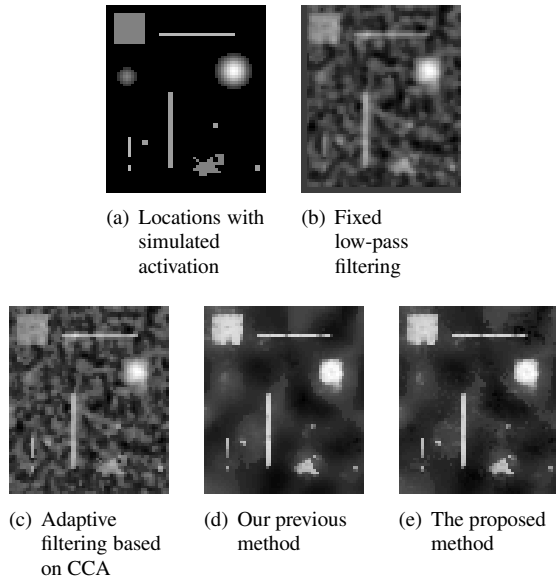


**Fig. 3.** Locations with simulated activity and active regions detected using the different analysis methods.

In figure 4, receiver operating characteristic (ROC) curves, showing the sensitivity (ability to correctly classify active voxels) versus the specificity (ability to correctly classify inactive voxels) of the different methods, are displayed.

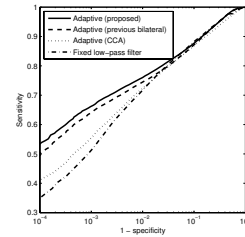
It is evident from the ROC curves that the methods based on bilateral filtering have superior ability to discriminate between active and inactive voxels in the simulated data. This is also supported by the correlation maps in figures 3d-e, which show sharper edges between active and inactive regions than the correlation maps generated by the CCA method and the method based on a fixed filter. This edge-preserving property is clearly an advantage of these methods. While the visible difference between the correlation map from our previous method and that from the proposed method is not very large, the ROC curves clearly show that the proposed inclusion of a second range filter, based on time-series similarity, provides a further enhancement of the detection performance. This is to be expected, since the new range filter reduces the risk of creating too large filters.

Figure 5 shows activation detected in real data from a finger tapping task, overlaid on an anatomical image of the brain. The activation in the motor cortex is consistent with the task.

Although the method is here presented for two-dimensional filtering, a generalization to three dimensions is straight-forward. Since three-dimensional filtering utilizes the correlations between neighboring slices, further improvements of the detection performance is expected.

## 5. CONCLUSION

A new method for adaptive filtering of fMRI data has been presented and evaluated. The method, which is based on bi-



**Fig. 4.** ROC curves for the different analysis methods. The proposed method provides the best detection performance.

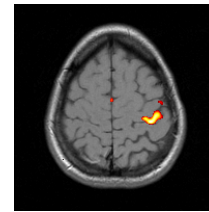


**Fig. 5.** Activation detected using the proposed method on real data from a finger tapping experiment. As expected, the detected activation resides in the motor cortex.

lateral filtering, extends our previous fMRI analysis scheme. Experimental results have shown that the new method provides improved activation detection performance.

## 6. REFERENCES

- [1] K.J. Friston, P. Jezzard, and R. Turner, "Analysis of functional MRI time-series," *Human Brain Mapping*, vol. 1, pp. 153–171, 1994.
- [2] O. Friman, M. Borga, P. Lundberg, and H. Knutsson, "Adaptive analysis of fMRI data," *NeuroImage*, vol. 19, no. 3, pp. 837–845, 2003.
- [3] J. Rydell, H. Knutsson, and M. Borga, "Correlation controlled adaptive filtering for fMRI data analysis," in *Proceedings of the 13th Nordic-Baltic conference on biomedical engineering and medical physics (NBC'05)*, Umeå, Sweden, June 2005, NBC.
- [4] F. Godtlielsen, E. Spjøtvoll, and J. S. Marron, "A nonlinear Gaussian filter applied to images with discontinuities," *Nonparametric Statistics*, vol. 8, pp. 21–43, 1997.
- [5] C. Tomasi and R. Manduchi, "Bilateral filtering for gray and color images," in *IEEE International Conference on Computer Vision 98*, Bombay, India, January 1998, IEEE, pp. 839–846.
- [6] F. Godtlielsen, C.-K. Chu, S. H. Sørbye, and G. Torheim, "An estimator for functional data with application to MRI," *IEEE Transactions on Medical Imaging*, vol. 20, no. 1, pp. 36–44, 2001.
- [7] R.B. Buxton, E.C. Wong, and L.R. Frank, "Dynamics of blood flow and oxygenation changes during brain activation: the Balloon model," *Magnetic Resonance in Medicine*, vol. 39, no. 6, pp. 855–864, 1998.